Mol Cell Toxicol (2012) 8:127-137
DOI 10.1007/s13273-012-0016-6

ORIGINAL PAPER

Gene expression in zebrafish embryos following exposure to Cu-doped TiO_2 and pure TiO_2 nanometer-sized photocatalysts

Min-Kyeong Yeo[1] **& Hyung-Geun Park**[1]

Received: 28 July 2011 / Accepted: 1 November 2011

Abstract We investigated the comparative effects of Cu 15 mol % doped TiO_2 (anatase crystal phase, 20 ppt) nanoparticles and pure TiO_2 (anatase crystal phase, 20 ppt) nanoparticles on cellular toxicity, penetration, and gene expression in zebrafish embryogenesis. HR-TEM analysis observed that pure TiO_2 particles were in the form of small balls (< 10 nm), while Cu-doped (15 mol %) TiO_2 particles were large (20-70 nm) squares and balls. Both Cu/TiO_2 and pure TiO_2 nanoparticles penetrated into cells. Cu/TiO_2 nanoparticles penetrated into the yolk sac epithelial cells of zebrafish larvae as aggregated particles. Mitochondria in embryos exposed to Cu/TiO_2 nanoparticles were damaged and did not contain cristae. In microarray analysis, several genes involved in apoptosis and endocytosis regulation were differentially expressed according to nanoparticle type. Bcl2 gene expression was significantly upregulated in embryos exposed to both Cu/TiO_2 and pure TiO_2 in comparison to the control group. Cu/TiO_2 nanoparticles caused more damage than pure TiO_2 nanoparticles and resulted in apoptosis during zebrafish development.

Keywords Nanometer-sized TiO_2, Cu doped TiO_2, Gene expression, Regulation endocytosis

Recent studies have focused on the degradation of organic and inorganic environmental pollutants by TiO_2 photocatalysis[1,2]. The addition of cations such as Pt, Cr^{3+}, Cu^{2+}, and Fe^{3+} into anatase TiO_2 can increase its photoactivity[3-7]. Cu-doped TiO_2 systems have potential as photocatalysts, and their photocatalytic potential improves with optimal Cu content[8].

Nano-sized pure TiO_2 has gained attention because it is an environmental toxin that is produced in large amounts for use as a self-cleaning, antimicrobial, and antifouling agent in paint[9-11]; and as a UV-absorber in cosmetics[12-15]. Synthetic nano-Ti from paint has been known to leach into small streams, resulting in concentrations of 2-3 $\mu g\ L^{-1}$ of nano-TiO_2 in bodies of water[16]. In Switzerland, model calculations estimating the release of nano-TiO_2 into the environment have been performed using substance flow analysis from various commercial products into air, soil, and water[17,18].

Many studies have documented the phototoxic and photo-genotoxic effects of TiO_2 (both normal and nano-sized)[19-23]. Consequently, its properties as a photo-catalytic compound have been applied to waste water disinfection[24] and photodynamic cancer therapy[25,26]. TiO_2 nanoparticle size increases to greater than 100 nanometers (nm) with the addition of a metal cation into an anatase TiO_2 nanoparticle. Particles smaller than 100 nm do not appear to be as toxic as larger particles, although there are several reports of Cu-induced toxicity in fish. Cu-induced ionoregulation in developing fish is initially exclusively transcutaneous[27-29]. Nanoparticles exposed to Cu/TiO_2 and pure TiO_2 showed an increase in the activity of several anti-oxidant enzymes in zebrafish larvae[30]. There are many uses for metal-doped TiO_2 nanoparticles, such as facilitating the inflow of Cu-doped TiO_2 nanoparticles into water. However there are a few studies describing Cu-doped TiO_2 nanoparticle biological toxicity and its impact on gene expression.

In the present study, we investigated the effects of Cu-doped (15 mol %) TiO_2 (anatase crystal phase, 20 ppt) nanoparticles and anatase TiO_2 nanoparticles (20

[1]Department of Environmental Science and Environmental Research Center, College of Engineering, Kyung Hee University, 1732 Deogyeong-daero, Giheung-gu, Yongin-si, Gyeonggi-do 446-701, Republic of Korea
Correspondence and requests for materials should be addressed to M.-K. Yeo (✉ bioclass@khu.ac.kr)

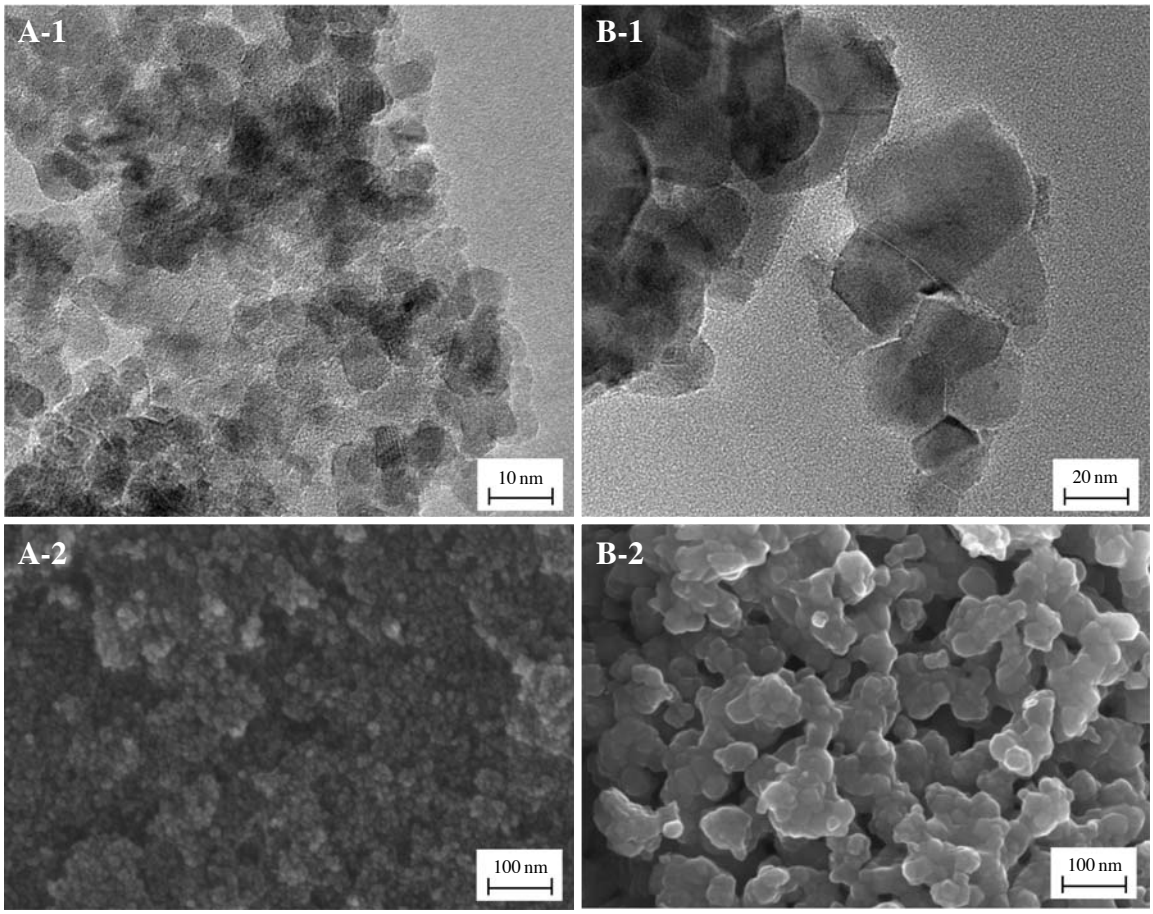

Figure 1. HR-TEM analysis and FE-SEM images of Cu/TiO_2 and pure TiO_2 nanoparticles. HR-TEM analysis: A-1) pure TiO_2 nanoparticles, B-1) Cu/TiO_2 nanoparticles. FE-SEM images: A-2) pure TiO_2 nanoparticles, B-2) Cu/TiO_2 nanoparticles.

ppt) on cellular toxicity, penetration, and gene expression in zebrafish embryogenesis.

Characterization of TiO_2 nanoparticles

We observed two different types of TiO_2 nanoparticles using HR-TEM analysis: type A-1, which was pure TiO_2, and type B-1, which was Cu-doped TiO_2 (Figure 1). Scanning electron microscope images showed that pure TiO_2 particles (Figure 1A-2) were shaped like small balls, while Cu-doped TiO_2 particles were shaped like squares and balls (Figure 1B-2). Pure TiO_2 particles were also generally smaller (< 15 nm) than Cu-doped TiO_2 particles (20-70 nm).

TEM analysis of embryos exposed to pure TiO_2 nanoparticles and Cu-doped TiO_2 nanoparticles

Embryonic cells were exposed to pure TiO_2 and Cu/TiO_2 nanoparticles, resulting in significant damage to the mitochondria (Figure 2). Pure TiO_2 and Cu/TiO_2 penetrated into the yolk sac epithelial cells of zebrafish larvae as aggregated particles (Figure 3). The particle size of pure TiO_2 increased approximately 60 nm. Cu/TiO_2 nanoparticles were more aggregated than pure TiO_2 nanoparticles.

Altered gene expression in zebrafish embryos exposed to pure TiO_2 nanoparticles and Cu-doped TiO_2 nanoparticles

Gene expression profiles were significantly up- or downregulated in embryos exposed to Cu/TiO_2 or pure TiO_2 nanoparticles when compared to embryos in the control group (Table 1).

Cu-doped and pure TiO_2 nanoparticles affected genes such as casp6l2, casp6l1, casp6, and tnfrsf19 in a variety of ways. Apoptosis-related genes such as casp8, casp6 and casp6l2 were upregulated ten times more frequently in embryos exposed to Cu/TiO_2 than in pure TiO_2 nanoparticle embryos.

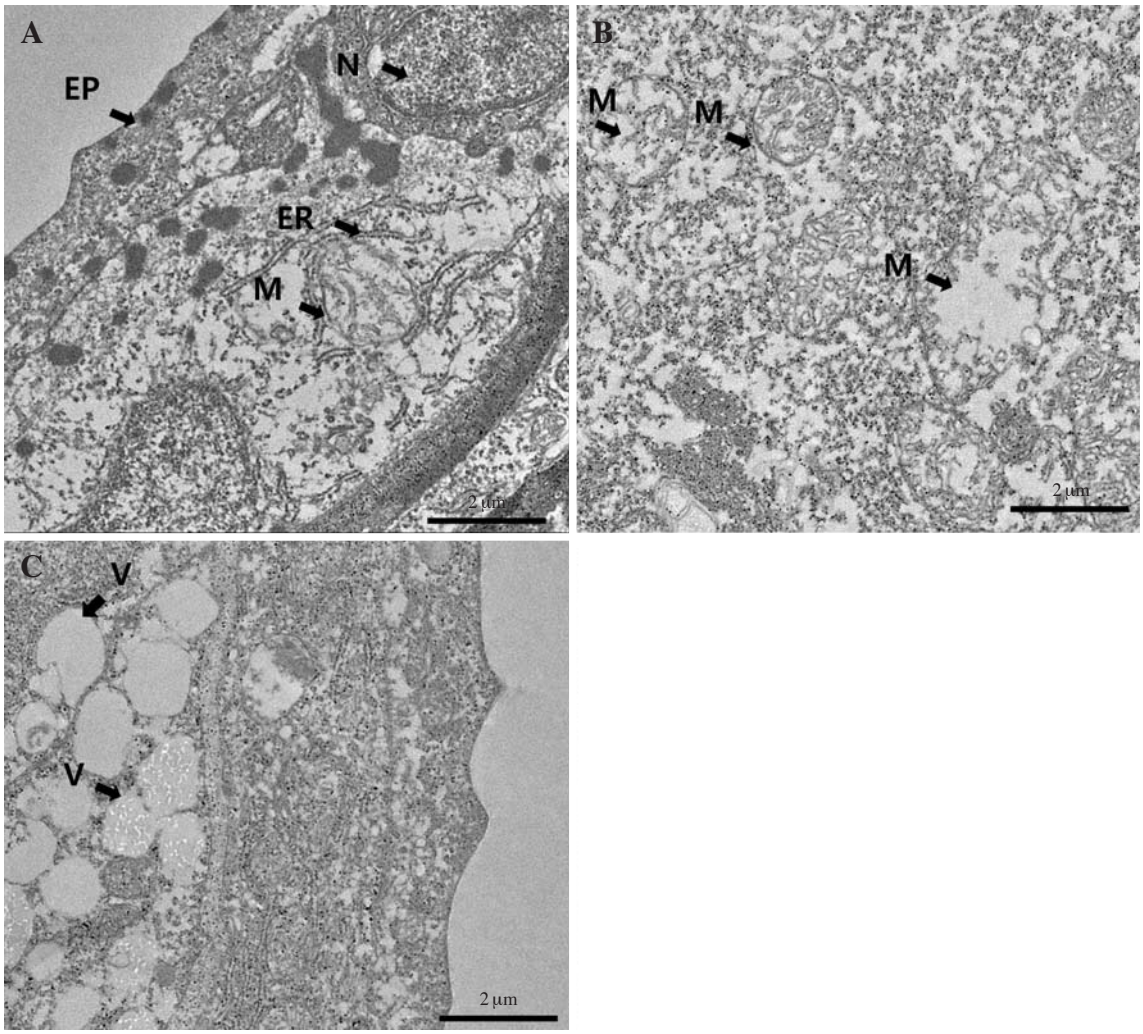

Figure 2. TEM images of zebrafish larvae after exposure to Cu-doped TiO_2 and pure TiO_2 nanoparticles. A; Control, B; pure TiO_2 nanoparticle, C; Cu-doped TiO_2 nanoparticle. Abbreviations: EP; epidermal tissue, ER; endocrine reticulum, N; nucleus, M; mitochondria, V; emptied vesicle.

Table 1. Analysis of genes with altered expression in zebrafish embryos exposed to Cu-doped TiO_2 and pure TiO_2 nanometer sized photocatalysts.

Gene description	Gene symbol	Regulation profile and ratio	
		TiO_2	Cu15%-TiO_2
Endocytosis			
Danio rerio RAB43, member RAS Oncogene family (rab43)	rab43	0.154887	0.760988
Danio rerio RAB5A, member RAS Oncogene family (rab5a)	rab5a	0.38463	0.752259
Danio rerio RAB11 family interacting protein 4 (class II) b (rab11fip4b)	rab11fip4b	0.357244	0.297409
Danio rerio limb region 1 like (lmbr1l)	lmbr1l	0.124391	0.965404
Danio rerio zgc:101777 (zgc:101777)	zgc:101777	0.351079	0.95208
SH3-domain binding protein 4			
Novel protein similar to H. sapiens EEA1, early endosome antigen 1 (EEA1) Fragment	CH211-204P6.5	4.79118	3.438632
Danio rerio EH-domain containing 3 (ehd3)	ehd3	10.7389	6.384697

Table 1. Continued.

Gene description	Gene symbol	Regulation profile and ratio	
		TiO_2	Cu15%-TiO_2
Novel protein similar to vertebrate phospholipase D family, member 3 (PLD3)	LOC799742	3.621709	1.986815
Danio rerio SH3-domain binding protein 4a (sh3bp4a) cell differentiation, phagocytosis	sh3bp4a	16.85771	6.790448
Danio rerio disabled homolog 2 (Drosophila) (dab2), apoptosis, phagocytosis	dab2	2.12898	1.46563
Danio rerio notch homolog 1a (notch1a)	notch1a	4.988464	4.174082
Danio rerio cadherin-like 23 (cdh23)	cdh23	2.422812	1.906827
Danio rerio si:ch211-197g15.3 (si:ch211-197g15.3)	si:ch211-197g15.3	1.00936	2.005045
Danio rerio myosin VIIa (myo7a)	myo7a	3.026458	9.629787
PREDICTED: *Danio rerio* similar to RAB11 family interacting protein 4 (class II) (LOC557691)	LOC557691	1.887949	3.403859
Danio rerio similar to EPS15 protein	LOC795505	1.825916	4.151695
Danio rerio mind bomb (mib)	mib	2.258887	2.130319
Danio rerio similar to signal peptide, CUB domain, EGF-like 1	LOC797832	2.154173	2.374888
Apoptosis			
Danio rerio caspase b (caspb)	caspb	0.461471	0.474625
PREDICTED: *Danio rerio* similar to caspase recruitment domain family, member 14 (LOC568689)	LOC100003058	0.108366	1.746996
Danio rerio caspase 8, apoptosis-related cysteine peptidase (casp8)	casp8	0.062175	1.084681
Danio rerio bcl2-like (bcl2l)	bcl2l	0.432902	0.745193
Danio rerio caspase 3, apoptosis-related cysteine protease b (casp3b)	casp3b	0.208687	0.646645
Danio rerio BH3 interacting domain death agonist (bida)	bida	0.31314	0.68006
Danio rerio bcl2-associated X protein, b (baxb)	baxb	0.335693	0.510809
Danio rerio caspase 7, apoptosis-related cysteine peptidase (casp7)	casp7	0.332594	1.061372
Danio rerio caspase a (caspa)	caspa	0.172641	0.576651
Danio rerio CASP2 and RIPK1 domain containing adaptor with death domain (cradd)	cradd	0.452306	0.182957
Danio rerio insulin-like growth factor 1a receptor (igf1ra)	igf1ra	0.17067	0.411022
Danio rerio caspase Xa (caspxa)	caspxa	0.325393	0.591764
Danio rerio tumor protein p53 binding protein, 2 (tp53bp2)	tp53bp2	0.476223	1.396359
Probable fructose-2,6-bisphosphatase TIGAR B (EC 3.1.3.46) (TP53-induced glycolysis and apoptosis regulator B)	tigarb	1.528997	0.449066
Danio rerio tp53-induced glycolysis and apoptosis regulator a (tigara)	tigara	0.532539	0.349164
Danio rerio CASP8 and FADD-like apoptosis regulator (cflar)	cflar	0.415116	0.262842
Danio rerio BCL2-interacting killer (apoptosis-inducing) (bik)	bik	0.697478	0.475424
Danio rerio zgc:63938 (zgc:63938)	zgc:63938	0.493138	0.416557
Danio rerio hematopoietic death receptor (hdr)	hdr	0.119536	0.164758
Danio rerio bcl2-associated X protein, a (baxa)	baxa	4.254227	4.105088
Danio rerio caspase 3, apoptosis-related cysteine protease a (casp3a)	casp3a	1.165585	0.750662
Danio rerio caspase b-like (LOC566185)	CH211-15J1.6	1.269702	1.656825
Danio rerio caspase 6, apoptosis-related cysteine peptidase, like 2 (casp6l2)	casp6l2	0.308785	12.49477
Danio rerio caspase 6, apoptosis-related cysteine peptidase, like 1 (casp6l1)	casp6l1	0.394353	2.867153

Table 1. Continued.

Gene description	Gene symbol	Regulation profile and ratio	
		TiO_2	Cu15%-TiO_2
Danio rerio caspase 6, apoptosis-related cysteine peptidase (casp6)	casp6	0.18482	2.754182
Danio rerio caspase c (caspc)	Caspc	8.945293	3.278705
PREDICTED: *Danio rerio* similar to Contactin-associated protein 1 precursor (Caspr) (Caspr1) (Neurexin 4) (Neurexin IV) (p190) (LOC566220)	LOC566220	14.12437	2.927776
Danio rerio B-cell leukemia/lymphoma 2 (bcl2)	bcl2	2.575752	1.485977
Danio rerio BCL2 binding component 3 (bbc3)	bbc3	1.722569	10.80311
PREDICTED: *Danio rerio* similar to caspase 7, apoptosis-related cysteine peptidase (LOC798445)	LOC798445	2.052208	2.526744
Danio rerio myeloid cell leukemia sequence 1a (mcl1a)	mcl1a	0.759528	3.764696
Danio rerio CASP8 and FADD-like apoptosis regulator (cflar)	Cflar	2.303582	3.972541
Danio rerio caspase 9, apoptosis-related cysteine protease (casp9)	casp9	1.166097	2.215856
Danio rerio similar to caspase c (LOC566600)	CH211-284E13.9	10.26673	11.93613
Danio rerio myeloid cell leukemia sequence 1b (mcl1b)	mcl1b	1.002413	2.476006
Tumor necrosis factor			
AGENCOURT_109127346 NIH_ZGC_30 *Danio rerio* cDNA clone IMAGE:9041794 5′	LOC561000	0.1502	1.294764
Danio rerio tumor necrosis factor (ligand) superfamily, member 10 like (tnfsf10l)	tnfsf10l	0.375399	0.422243
Novel protein similar to vertebrate disintegrin and metalloproteinase domain 17 (Tumor necrosis factor, alpha, converting enzyme) (ADAM17) Fragment	adam17b	0.199734	1.317744
Danio rerio Fas ligand (TNF superfamily, member 6) (faslg)	faslg	0.478062	1.36101
Danio rerio tumor necrosis factor receptor superfamily, member 19 (tnfrsf19)	tnfrsf19	0.429791	1.874813
Danio rerio tumor necrosis factor (ligand) superfamily, member 10 like 4 (tnfsf10l4)	tnfsf10l4	0.026749	0.75901
Novel protein similar to vertebrate disintegrin and metalloproteinase domain 17 (Tumor necrosis factor, alpha, converting enzyme) (ADAM17) Fragment	adam17b	0.199734	1.317744
Danio rerio tumor necrosis factor (ligand) superfamily, member 10 like 2 (tnfsf10l2)	tnfsf10l2	0.1487	0.292084
Danio rerio zgc:172115 (zgc:172115)	zgc:172115	0.912659	0.317095
Danio rerio tumor necrosis factor, alpha-induced protein 8, like (tnfaip8l)	tnfaip8l	0.225528	0.181652
Danio rerio tumor necrosis factor receptor superfamily, member 1a (tnfrsf1a)	tnfrsf1a	0.403525	0.408072
AGENCOURT_16543267 NIH_ZGC_10 *Danio rerio* cDNA clone IMAGE:7041153 5′	LOC797618	2.130541	1.66502
Danio rerio tumor necrosis factor b (TNF superfamily, member 2) (tnfβ)	tnfβ	2.355006	0.867605
Danio rerio lymphotoxin alpha (TNF superfamily, member 1) (lta)	lta	2.228476	1.776712
Danio rerio tumor necrosis factor receptor superfamily, member 21 (tnfrsf21)	tnfrsf21	1.045915	3.389496
Danio rerio tumor necrosis factor receptor superfamily, member 1a (tnfrsf1a)	tnfrsf1a	20.7781	4.229965
Danio rerio C1q and tumor necrosis factor related protein 4 (c1qtnf4)	c1qtnf4	2.006739	9.764094

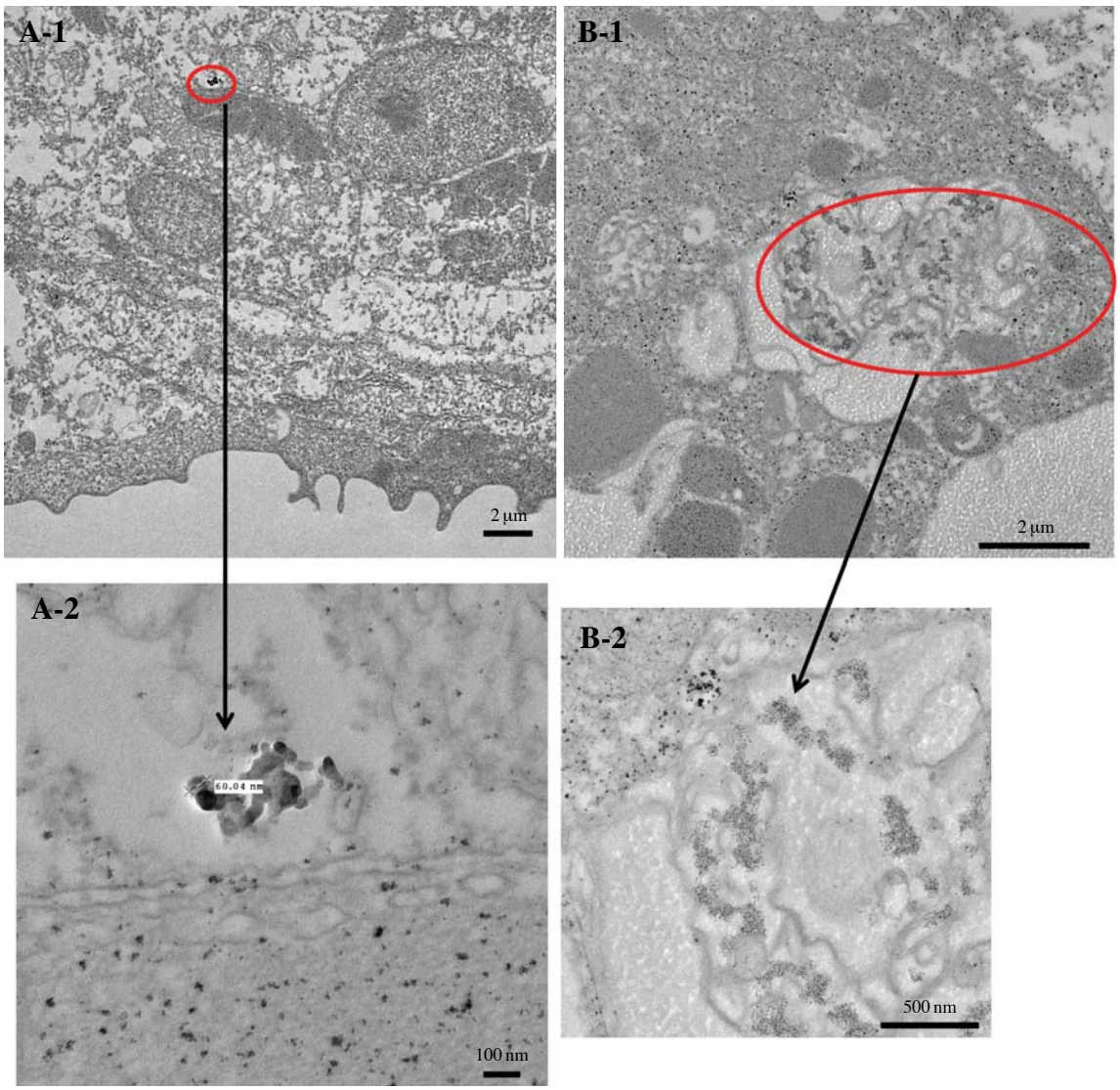

Figure 3. TEM images of aggregated Cu-doped TiO_2 and pure TiO_2 nanoparticles in the cell. A-1; pure TiO_2 nanoparticle, A-2; in the circle of A, B-1; Cu doped TiO_2 nanoparticle, B-2; in the circle of B-1.

When compared to the control group, embryos exposed to Cu/TiO_2 and pure TiO_2 nanoparticles exhibited upregulation in endocytosis-related gene expression. However, exposure to Cu/TiO_2 and pure TiO_2 resulted in downregulation of gene expression in members of the RAS oncogene family, including rab43, rab5a, rab43 and rab11fip4b.

Tumor necrosis factor superfamily genes (tnfrsf21, tnfrsf19) demonstrated significant upregulation in embryos exposed to Cu/TiO_2 nanoparticles (Table 2), when compared to pure TiO_2 nanoparticles. Expression of the tigarb gene, which is related to tp53-induced glycolysis and apoptosis regulator b in Cu/TiO_2 nanoparticle exposed embryos, was downregulated when compared to embryos exposed to the pure TiO_2 nanoparticles.

Discussion

This study evaluated cellular toxicity and gene expression in Cu-doped TiO_2 and pure TiO_2 nanoparticles. Mitochondria in embryos exposed to Cu/TiO_2 appeared to be severely damaged, as no cristae were observed (Figure 2C). Embryos exposed to pure TiO_2 were also damaged, although cristae were still present (Figure 2B).

Our results are consistent with previous findings

Table 2. Comparative analysis of genes with altered expression in zebrafish embryos exposed to Cu doped TiO_2 and pure TiO_2 nanoparticles.

Gene name, Description	Gene symbol	Cu 15%-TiO_2
RAB43, member RAS oncogene family	rab43	4.913189
tumor necrosis factor, alpha-induced protein 8, like	tnfaip8l	11.40609
similar to EPS15 protein	LOC795505	2.27376
disabled homolog 2 (Drosophila)	dab2	2.790189
caspase 3, apoptosis-related cysteine protease b	casp3b	3.098633
caspase 7, apoptosis-related cysteine peptidase	casp7	3.191199
caspase 8, apoptosis-related cysteine peptidase	casp8	17.44562
caspase 6, apoptosis-related cysteine peptidase	casp6	14.90195
tumor protein p53 binding protein, 2	tp53bp2	2.932155
similar to tumour necrosis factor receptor	LOC561000	8.620286
similar to TNFAIP3 interacting protein 1	LOC100004948	9.676461
similar to tumour necrosis factor receptor	LOC561000	8.620286
Fas ligand (TNF superfamily, member 6)	faslg	2.846932
BH3 interacting domain death agonist	bida	2.171747
BCL2 binding component 3	bbc3	3.248176
similar to caspase recruitment domain protein 14	LOC100003058	16.12128
a disintegrin and metallopeptidase domain 17b	adam17b	6.597482
limb region 1 like	lmbr1l	7.761042
myosin VIIa	myo7a	3.181868
RAB43, member RAS oncogene family	rab43	4.430992
myeloid cell leukemia sequence 1a	mcl1a	4.956628
tumor necrosis factor receptor superfamily, member 21	tnfrsf21	3.240701
tumor necrosis factor receptor superfamily, member 19	tnfrsf19	4.362145
caspase 3, apoptosis-related cysteine protease b	casp3b	3.098633
caspase 8, apoptosis-related cysteine peptidase	casp8	17.44562
tumor necrosis factor (ligand) superfamily, member 10 like	tnfsf10l	7.185313
myeloid cell leukemia sequence 1b	mcl1b	2.470045
tumor necrosis factor (ligand) superfamily, member 10 like 4	tnfsf10l4	28.37522
SH3-domain binding protein 4a	sh3bp4a	2.228907
caspase 6, apoptosis-related cysteine peptidase, like 2	casp6l2	40.46425
C1q and tumor necrosis factor related protein 4	c1qtnf4	4.865651
caspase 6, apoptosis-related cysteine peptidase, like 1	casp6l1	7.270519
caspase b	caspb	5.620031
insulin-like growth factor 1a receptor	igf1ra	2.602846
caspase c	caspc	0.366529
zgc:172115	zgc:172115	0.347441
tumor necrosis factor receptor superfamily, member 1a	tnfrsf1a	0.203578
similar to Contactin-associated protein 1 precursor (Caspr) (Caspr1) (Neurexin 4) (Neurexin IV) (p190)	LOC566220	0.207285
CASP2 and RIPK1 domain containing adaptor with death domain	cradd	0.404498
tumor necrosis factor (ligand) superfamily, member 10 like 2	tnfsf10l2	0.286456
mind bomb 2	mib2	0.130185
similar to Disabled homolog 2 (Differentially-expressed protein 2) (DOC-2)	LOC797982	0.184742
SH3-domain binding protein 4a	sh3bp4a	0.40281
zgc:172115	zgc:172115	0.38303
tumor necrosis factor b (TNF superfamily, member 2)	tnfb	0.368409
tp53-induced glycolysis and apoptosis regulator b	tigarb	0.2937
zgc:172115	zgc:172115	0.347441
tp53-induced glycolysis and apoptosis regulator b	tigarb	0.2937
Fas (tnfrsf6)-associated via death domain	fadd	0.329732

showing that metals such as Cu are toxic to aquatic organisms, even at low concentrations[31]. The co-existence of nanoparticles with Cu^{2+} raises concerns about the enhanced biotoxicity of Cu^{2+} [31].

Both Cu/TiO_2 and pure TiO_2 nanoparticles aggregated in the cell (Figure 3), but the Cu/TiO_2 nanoparticles penetrated into the epithelium cells of zebrafish larvae as aggregated particles (Figure 3B-2). These results are similar to the findings of previous studies[11].

We showed that nanoparticles induce adverse biological responses in the mitochondria of zebrafish larvae. These results are consistent with previous studies that found damaged mitochondria-rich cells (MRCs) have abnormal ionic regulation and are involved in Ca^{2+} [32], Na^{+} [33] uptake. MRCs also appear to be responsible for proton secretion[34] in zebrafish at an early age[35]. ATP is typically produced by mitochondria, but damaged mitochondria lose this ability. Damaged mitochondria also appear to cause cell apoptosis by causing the outer membrane pores to release cytochrome C[36].

Our results revealed that expression of the Bcl2 gene in groups exposed to Cu/TiO_2 (1.486) and pure TiO_2 (2.58) nanoparticles was higher than in the control group (Table 1). Expression of the Baxa gene is also higher in both pure TiO_2 (4.254227) and Cu/TiO_2 (4.105088). That said, expression of tp 53bp2 (tumor protein p53 binding protein 2) was only higher in the group exposed to Cu/TiO_2 (1.396). These data confirm previous observations that Bcl-2 family members either reside or congregate on mitochondria and other organelles during apoptosis[36]. The Bcl-2 family regulates an ancient path to cell death, and this diverse family of proteins falls into three distinct groups. Bcl-2 and several close relatives inhibit apoptosis[37], whereas structurally similar relatives such as Bax[38] and distant cousins such as Bik and Bim[39] induce apoptosis.

There are two kinds of competitive energy that are important for the endocytosis of nanoparticles (NPs). One is the binding energy between ligands and receptors, and the other is the thermodynamic driving force behind wrapping[40]. Our results revealed that embryos exposed to Cu/TiO_2 and pure TiO_2 nanoparticles exhibited upregulation in endocytosis-related gene expression when compared to the control group. Cu/TiO_2 and pure TiO_2 nanoparticles are the types of ligands bind to receptors in the cell the suggestion require further study.

We showed that Cu/TiO_2 and pure TiO_2 nanoparticles cause mitochondrial damage in zebrafish. Cu/TiO_2 nanoparticles appear to cause more severe damage than pure TiO_2 nanoparticles and result in apoptosis in zebrafish larvae.

Materials & Methods

Characteristics of TiO_2 and Cu/TiO_2 nano-sized photocatalysts

TiO_2 and Cu/TiO_2 nano-sized photocatalysts were kindly donated by Misook Kang, Young Nam University, Korea. A high resolution transmission electron microscope (HRTEM, JEOL, Japan) with an accelerating voltage of 300 kV was used to study the structures and morphologies of TiO_2 and Cu/TiO_2 nano-sized photocatalysts. The samples were placed on copper grids for TEM imaging. TiO_2 and Cu/TiO_2 powders were subjected to X-ray diffractometer (XRD, model PW 1830; Philips, Amsterdam, The Netherlands) with nickel-filtered CuK radiation (30 kV, 30 mA) at 2θ angles from 5° to 70°, with a scan speed of 10° min^{-1} and time constant of 1s. The sizes and shapes of TiO_2 and Cu/TiO_2 particles were observed using scanning electron microscopy (SEM, model JEOL-JSM35CF; Tokyo, Japan) with the power set to 15 kV.

Experimental animals

The zebrafish (*Danio rerio*, wild-type) used in this study were bred in our laboratory and were approximately 7-8 months old. Fish were cared for in accordance with standard zebrafish protocols[41] approved by the Animal Care and Use Committee of Kyung Hee University. Experimental animals were housed in a 60-L glass tank with a carbon filter. The water temperature was maintained at 28 ± 1°C with a 14/10 h light/dark cycle. Adult fish were maintained on a diet of bloodworms, dry flake food, and brine shrimp. Eggs were laid and fertilized within one hour of the beginning of the light cycle, which resulted in large samples of synchronously developing embryos. The embryos were collected, pooled, and rinsed several times. Embryonic staging was carried out according to the standardized staging series established by Kimmel *et al.*[42] The embryos were immersed in exposure or vehicle control solutions at the 64- to 256-cell stages and at 2.5 hours post-fertilization. Dead embryos were removed to avoid contamination of the test solutions. Embryos were observed with a microscope (Olympus, SZ61, Japan) to determine the effects of exposure to Cu-doped TiO_2 nanoparticles and TiO_2 nanoparticles.

Chemical exposure during development

Cu/TiO_2 and TiO_2 nanoparticles were suspended in city water that was allowed to stand for 24 hours to evaporate chlorine, as recommended in previous research[43]. The final nanoparticle exposure concentrations were 20 ppt in each group (TiO_2 and Cu/TiO_2).

Each group of embryos was placed in 1-L glass beakers and maintained in a carbon-filtrated water system at $28 \pm 1^{\circ}C$. Each group contained 300 viable embryos. Embryos were randomly divided into the following groups: Group 1 embryos made up the control group; Group 2 embryos were exposed to TiO_2 nanoparticles, and Group 3 embryos were exposed to Cu-doped (15 mol %) TiO_2 nanoparticles. Embryos were observed at 4, 8, 22, 27, 32, 48, 52, and 72 hours post-fertilization (hpf), which are time points based on known developmental stages[29]. Dead embryos were removed during development. The hatched embryos at 72 hpf were investigated using TEM and Microarray analysis.

Histological preparation and transmission electron microscopy (TEM)

Tissue were fixed at 4°C in 2% glutaraldehyde in sodium phosphate buffer, post fixed in 1% osmium tetroxide, dehydrated through graded ethanol solutions and then embedded in Embed 812-Araldite 502 resin (EMS). For transmission electron microscopy, ultrathin sections (60 to 70 nm of depth) were mounted on copper grids and then stained in lead citrate and uranyl acetate solutions for examination. The sample observed using a field emission transmission electron microscope (FE TEM, H-7600, operated at 80 kV, Hitachi, Japan).

Microarray analysis

RNAs from Zebrafish embryo were rapidly isolated by zebrafish book method[41].

For control and test RNAs, the synthesis of target cRNA probes for hybridization was performed using Agilent's Low RNA Input Linear Amplification kit PLUS (Agilent Technology; USA) according to the manufacturer's instructions. T7 promoter primer mix and one μg total RNA and were incubated at 65°C for ten minutes. The cDNA master mix (5X first strand buffer, 0.1 M DTT, 10 mM dNTP mix, RNase-Out, and MMLV-RT) was prepared and added to the reaction mixer. Samples were incubated at 40°C for two hours and then the RT and dsDNA syntheses were terminated by incubating at 65°C for 15 minutes. The transcription master mix was prepared according to the manufacturer's protocol (4X transcription buffer, 0.1 M DTT, NTP mix, 50% PEG, RNase-Out, Inorganic pyrophosphatase, T7-RNA polymerase, and Cyanine 3-CTP). The transcription of dsDNA was performed by adding transcription master mix to the dsDNA reaction samples and incubating at 40°C for two hours. Amplified and labeled cRNA was purified with the cRNA Cleanup Module (Agilent) according to the manufacturer's protocol. The labeled cRNA target was quantified using a ND-1000 spectrophotometer (NanoDrop Technologies, Inc.; Wilmington, DE, USA). After checking the labeling efficiency, cRNA fragmentation was performed by adding 10X blocking agent and 25X fragmentation buffer and incubating at 60°C for 30 minutes. The fragmented cRNA was resuspended with 2X hybridization buffer and directly pipetted onto an assembled Agilent Zebrafish Oligo Microarray Kit V2 (44K). The arrays were hybridized at 65°C for 17 hours using a hybridization oven (Agilent). The hybridized microarrays were washed according to the manufacturer's washing protocol.

Data acquisition and analysis

The hybridized images were scanned using an Agilent Microarray Scanner (Agilent #G2565BA) and quantified with Feature Extraction Software (Agilent). All data normalization and selection of fold-changed genes were performed using GeneSpringGX 7.3 (Agilent). Intensity-dependent normalization (LOWESS) was performed, and the ratio was reduced to the residual of the Lowess fit of the intensity vs. ratio curve. The averages of normalized ratios were calculated by dividing the average of the normalized signal channel intensity by the average of the normalized control channel intensity. Functional annotation of genes was performed according to the Gene Ontology™ Consortium (http://www.geneontology.org/index.shtml) by GeneSpringGX 7.3. Gene classification was conducted based on searches performed using BioCarta (http://www.biocarta.com/), GenMAPP (http://www.genmapp.org/), DAVID (http://david.abcc.ncifcrf.gov/), and Medline databases (http://www.ncbi.nlm.nih.gov/).

Acknowledgements This research was supported by Basic Science Research Program through the National Research Foundation of Korea (NRF) funded by the Ministry of Education, Science and Technology (2011-0022852).

References

1. Sreethawong, T., Suzuki, Y. & Yoshikawa, S. Photocatalytic evolution of hydrogen over nanocrystalline mesoporous titania prepared by surfactant-assisted templating sol-gel process. *Catal Commun* **6**:119-124 (2005).
2. Ho, W., Yu, J. C. & Yu, J. Photocatalytic TiO_2/glass nanoflake array films. *Langmuir* **21**:3486-3492 (2005).
3. Kim, S., Hwang, S. & Choi, W. Visible light active platinum-ion-doped TiO_2 photocatalyst. *J Phys Chem B* **109**:24260-24267 (2005).
4. Kemp, T. J. & McIntyre, R. A. Transition metal-doped titanium (IV) dioxide: characterisation and influence

on photodegradation of poly (vinyl chloride). *Polym Degrad Stabil* **91**:165-194 (2006).
5. Tseng, I. H., Wu, J. C. S. & Chou, H. Y. Effects of sol-gel procedures on the photocatalysis of Cu/TiO_2 in CO_2 photoreduction. *J Catal* **221**:432-440 (2004).
6. Li, Z., Shen, W., He, W. & Zu, X. Effect of Fe-doped TiO_2 nanoparticle derived from modified hydrothermal process on the photocatalytic degradation performance on methylene blue. *J Hazard Mater* **155**:590-594 (2008).
7. Janes, R., Knightley, L. J. & Harding, C. J. Structural and spectroscopic studies of iron (III) doped titania powders prepared by sol-gel synthesis and hydrothermal processing. *Dyes Pigments* **62**:199-212 (2004).
8. Choi, H. J. & Kang, M. Hydrogen production from methanol/water decomposition in a liquid photosystem using the anatase structure of Cu loaded TiO_2. *Int J Hydrogen Energy* **32**:3841-3848 (2007).
9. Moore, M. Do nanoparticles present ecotoxicological risks for the health of the aquatic environment? *Environ Int* **32**:967-976 (2006).
10. Lovern, S. B. & Klaper, R. *Daphnia magna* mortality when exposed to titanium dioxide and fullerene (L_{60}) nanoparticles. *Environ Toxicol Chem* **25**:1132-1137 (2006).
11. Daughton, C. G. Non-regulated water contaminants: emerging research. *Environ Impact Asses Rev* **24**:711-732 (2004).
12. NanoRoad. Overview of Promising Nanomaterials for Industrial Applications. (URL: http://www.nanoroad.net/download/overviewnanomaterials.pdf) (2005).
13. American Elements. Silver Nanoparticles. (URL: http://www.americanelements.com/agnp.html) (2007).
14. Nanoscale. NanoActive Titanium Dioxide. (URL: http://www.nanoscalecorp.com/producvts and services/specialty chemicals/metal oxides/?page=tio2) (2007).
15. Chen, X. & Mao, S. S. Titanium dioxide nanomaterials: synthesis, properties, modifications, and applications. *Chem Rev* **107**:2891-2959 (2007).
16. Kaegi, R. *et al*. Synthetic TiO_2 nanoparticle emission from exterior facades into the aquatic environment. *Environ Pollut* **156**:233-239 (2008).
17. Mueller, N. & Nowack, B. Exposure modeling of engineered nanoparticles in the environment. *Environ Sci Technol* **42**:4447-4453 (2008).
18. Sharma, V. K. Aggregation and toxicity of titanium dioxide nanoparticles in aquatic environment - A Review. *J Environ Sci Heal A* **44**:1485-1495 (2009).
19. Jha, A. N. Genotoxicological studies in aquatic organisms: an overview. *Mut Res* **552**:1-17 (2004).
20. Huovinen, P. S., Penttila, H. & Soimasuo, M. R. Penetration of UV radiation into Finish lakes with different characteristics. *Int J Circumpolar Health* **59**:15-21 (2000).
21. Tedetti, M. & Sempere, R. Penetration of ultraviolet radiation in the marine environment. A review. *Photochem Photobiol* **82**:389-397 (2006).
22. Hader, D. P. & Sinha, R. P. Solar ultraviolet radiation-induced DNA damage in aquatic organisms: potential environmental impact. *Mutat Res* **571**:221-233 (2005).
23. Reeves, J. F., Davies, S. J., Dodd, N. J. F. & Jha, A. N. Hydroxyl radicals ($^{\cdot}OH$) are associated with titanium dioxide (TiO_2) nanoparticle-induced cytotoxicity and oxidative DNA damage in fish cells. *Mutation Research/Fundamental and Molecular Mechanisms of Mutagenesis* **640**:113-122 (2008).
24. Raisuddin, S. & Jha, A. N. Relative sensitivity of fish and mammalian cells to sodium arsenate and arsenite as determined by alkaline single cell gel electrophoresis and cytokinesis block micronucleus assay. *Environ Mol Mutagen* **44**:83-89 (2004).
25. Bols, N. C., Ganassin, R. C., Tom, D. J. & Lee, L. E. Growth of fish cell lines in glutamine-free media. Cytotechnology **16**:159-166 (1994).
26. Moore, M. N., Allen, J. I. & McVeigh, K. Environmental prognostics: an integrated model supporting lysosomal stress responses as predictive biomarkers of animal health status. *Mar Environ Res* **61**:278-304 (2006).
27. Alderdice, D. F. Osmotic and ionic regulation in teleost eggs and larvae. *Fish Physiol Biochem* **11**:163-251 (1988).
28. Rombough, P. J. Gas exchange, ionoregulation and the functional development of the teleost gill. *Am Fish Soc Symp* **40**:47-83 (2004).
29. Varsamos, S., Nebel, C. & Charmantier, G. Ontogeny of osmoregulation in postembryonic fish: a review. *Comp Biochem Physiol A* **141**:401-429 (2005).
30. Yeo, M. K. & Kang, M. S. Effects of Cu_xTiO_y nanometer particles on biological toxicity during zebrafish embryogenesis. *Korean J Chem Eng* **26**:711-718 (2009).
31. Fan, W. *et al*. Nano-TiO_2 enhances the toxicity of copper in natural water to *Daphnia magna*. *Environ Pollut* **159**:729-734 (2011).
32. Pan, T. C., Liao, B. K., Huang, C. J., Lin, L. Y. & Hwang, P. P. Epithelial Ca^{2+} channel expression and Ca^{2+} uptake in developing zebrafish. *Am J Physiol Regul Integr Comp Physiol* **289**:1202-1211 (2005).
33. Esaki, M. *et al*. Visualization in zebrafish larvae of Na^+ uptake in mitochondria-rich cells whose differentiation is dependent on foxi3a. *Am J Physiol* **292**:470-480 (2007).
34. Lin, L. Y., Horng, J. L., Kunkel, J. G. & Hwang, P. P. Proton pump-rich cell secretes acid in skin of zebrafish larvae. *Am J Physiol Cell Physiol* **290**:371-378 (2006).
35. Jonz, M. G. & Nurse, C. A. Epithelial mitochondria-rich cells and associated innervation in adult and developing zebrafish. *J Comp Neurol* **497**:817-832 (2006).
36. Adams, J. M. & Cory, S. Life-or-death decisions by the Bcl-2 protein family. *Trends Biochem Sci* **26**:61-66 (2001).
37. Vaux, D. L. Bcl-2 gene promotes haemopoietic cell survival and cooperates with c-myc to immortalize pre-B cells. *Nature* **335**:440-442 (1988).
38. Gross, A., McDonnell, J. M. & Korsmeyer, S. J. Bcl-

2 family members and the mitochondria in apoptosis. *Genes Dev* **13**:1899-1911 (1999).
39. Kelekar, A. & Thompson, C. B. Bcl-2 homology domains: the role of the BH3 domain in apoptosis. *Trends Cell Biol* **8**:324-329 (1998).
40. Wang, S. H., Lee, C. W., Chiou, A. & Wei, P. K. Size-dependent endocytosis of gold nanoparticles studied by three-dimensional mapping of plasmonic scattering images. *J Nanobiotechnology* **8**: 3 (2010).
41. Westerfield, M. The Zebrafish book: A Guide for the Laboratory Use of Zebrafish (*Danio rerio*). University of Oregon Press, Eugene (2000).
42. Kimmel, C. B., Ballard, W. W., Kimmel, S. R., Ullmann, B. & Schilling, T. F. Stages of embryonic development of the zebrafish. *Dev Dyn* **203**:253-310 (1995).
43. Yeo, M. K. & Kang, M. S. Effects of nanometer sized silver materials on biological toxicity during zebrafish embryogenesis. *Bull Korean Chem Soc* **29**:1179-1184 (2008).